Laser-based Fragmentation of Microparticles for Nanoparticle Generation

Ramin Sattari, Christian Dieling, Stephan Barcikowski, and Boris Chichkov

Laser Zentrum Hannover e. V., Nanomaterials Group
Hollerithallee 8, 30419 Hannover, Germany
E-mail: s.barcikowski@lzh.de

Laser-based fragmentation of microparticles is a versatile method to generate engineered nanoparticles. The method allows a direct scaling and production of nanoparticle fractions and a continuous variation of the particle size by online control of the process and laser parameters without any chemical precursors. Especially properties like easy-to-clean and scratch-resistance surfaces, bioactivity and low-voltage electrical conductivity for microelectronics can have a potential effect on a growing existing market share of the automotive, medical engineering, electronics and optics branches. Due to the demand, ceramic (ZrO_2, Al_2O_3) and metal (Cu, Ti) micro powders have been selected for the study. The nanoparticles are formed by laser cracking submicron particles carried in a constant gas stream using a nanosecond Nd:YAG laser (λ = 532 nm). The influences of process parameters (pulse energy, gas type) on the particle size distribution and productivity of engineered nanoparticles will be examined. The size distribution of the engineered nanoparticles is determined by an online cascade impactor.

DOI: 10.2961/jlmn.2008.02.0008

Keywords: Pulsed laser ablation, Nanoparticles, Microparticles, Fragmentation

1. Introduction

Nano-particulate material products form a rapidly growing sector of the nanotechnology market, with a market share of 23% (volume of 15 billion EUR in 2002) [1]. The number of large and small start-up companies which are dealing with nano-particulate materials is growing exponentially, which reflects the demand for nano-materials for new endproducts. This is especially true for the automotive, medicine, cosmetics, electronics, and optics branches.

Currently, conventional techniques for bottom-up methods like wet chemistry, flame synthesis, and chemical gas phase synthesis are used for nanoparticle generation. The main disadvantages of these technologies are the necessity of chemical precursors and limitations in material choice.

Conventional top-down methods are mechanical milling and grinding, which are also limited by tool wear and contaminations through the milling tools, in particular, when abrasive materials like ceramics are used [2].

Compared to these techniques, laser-based generation of nanoparticles combine several properties, like wide-range material choice, no chemical precursors, and possibility of online monitoring of the particle size distribution during processing [3, 4]. Promising laser-based method for nanoparticle generation is the so-called laser ablation of microspheres (LAM), because of the scalability of the quality and the productivity of nanoparticles. New nano products, especially for medical applications, require high purity of the nanoparticles and scalable size distribution range effecting their specific properties of nanoscaled materials. Refining micron particles to form nanoparticles using the LAM process allows a control of the particle size distribution by varying the process parameters such as pulse energy, laser fluence, and type of gas [5].

It was reported that the laser ablation efficiency (in $\mu m^3/J$) can be optimized when using nanosecond pulses instead of picosecond pulses and when using shorter wavelengths (second or fourth harmonics) and smaller laser spot size [6]. But there are still deficits in the understanding of influences of the laser parameters and the type of gas inside the ablation chamber on the refinement of submicron-particles. These issues will be addressed in this paper.

2. State of the art

Laser ablation and fragmentation of microparticles (LAM) in the gas flow has been found to be a versatile method for the generation of nanoparticles [7, 8, 9, 10].

Previous results on laser ablation of permalloy, gold and silver microparticles (particle size $\approx$ 2 µm) by pulsed excimer laser (λ=248 nm; pulse-width of 12 ns) showed a mean particle diameter in the range from 10 to 100 nm, and a log-normal particle size distribution. Decreasing the laser fluence (from 5.4 to 2.2 J/cm² (Ag) and from 10 to 3.1 J/cm² (Au)) generally decreases the mean particle size from nearly 57 nm to 8.9 nm (Ag) and from nearly 116 nm to 82 nm (Au) [8]. Different to particle ablation from bulk material the threshold laser fluence is lower for microparticles [9].

The LAM process is also influenced by the photomechanical mechanism associated with the shock-wave propagation inside the microparticle. During the laser-assisted cracking of microparticles strong shock-wave formation in single particles has been observed in the velocity range of 1000-4000 m/s, even at near-threshold fluences [11]. With regard to the formulation of the mechanical relaxation time, this time depends on the size of the heating volume of a raw particle.

It was reported that the mean nanoparticle sizes produced by the process could be controlled using appropriate gas type (for example: helium, nitrogen, argon) and pressure (0.5, 1, 2 atm) [5]. The type of gas atmosphere influences the final size distribution (affecting the cooling rate). A smaller mean diameter of silver nanoparticles was detected when using argon (50 nm), compared to air as ambient gas (70-80 nm) under the same conditions (1 atm; F = 5.4 J/cm²). When argon is used as gas type the particle mean size increases much lower with the increase of the gas pressure compared to nitrogen [5].

The efficiency of LAM process for the generation of nanoparticles in gaseous media found to be quite acceptable even though the production of large quantities of primary nanoparticles using the LAM method was observed to be problematic, because of particle agglomeration in the ablation region, when no additional pressured air is supplied via a nozzle. The particle size distribution of cobalt particles can be shifted to the sub-100 nm-region reaching a maximum at 50 nm of the particle number concentration [4]. In [8] it was demonstrated that there is at least 10-50% mass conversion of permalloy feedstock material to nanoparticles. But the LAM process efficiency is not demonstrated for a wide range of different materials like ceramics and also for metals.

This paper addresses the influences of pulse energy and type of gas inside the process chamber on the productivity and particle size distribution of nanoparticles using laser cracking of micron and submicron particles.

Feedstock materials have been used, which are of high market interest for nano-end-products. Two ceramics, ZrO_2 and Al_2O_3, were chosen, since in previous investigations they show high potential for easy-to-clean and scratch-resistant surface technologies [12, 13, 14, 15], for example, for car body [16]. The metallic Cu is useful for various applications like catalysts, lubricants, environment sensors and electronic materials [8], and Ti has bioactive (proliferative) properties, which are used for medical technologies (stents, catheters) [1].

3. Experimental Set-up

The layout of the experimental set-up is shown in figure 1. The main components of the set-up are the Q-switched Nd:YAG laser (Gemini PIV120-15 with a wavelength of 532 nm, a maximum pulse energy of 120 mJ, a pulse repetition rate of 15 Hz, and a pulse duration of 3-5 ns), a gas-tight process chamber, a self-constructed micro-powder disperser, an online low pressure cascade impactor (with a particle size measurement range of 6 µm down to 14 nm, measuring the particle number concentration in $1/cm^{-3}$), and a vacuum pump. The vacuum pump generates a constant flow rate of 10.2 l/min, as required for the electrical low pressure cascade impactor (ELPI). The ELPI allows a quasi-continuous measurement (measurement frequency = 1 Hz) of the particle number concentration and size distribution during a laser ablation process. Furthermore, the flow rate of the ELPI is adequate for the flow requirement of the experimental set-up (fig. 1). Compared to mobility analyzer the aerodynamic diameter of primary nanoparticles is measured. The impacted nanoparticles on Aluminum-folio can be used for further analysis like SEM or EDX. Mobility analyzer have a higher size resolution with more than 30 size classifications and is usually be used for environmental and workplace measurements [17].

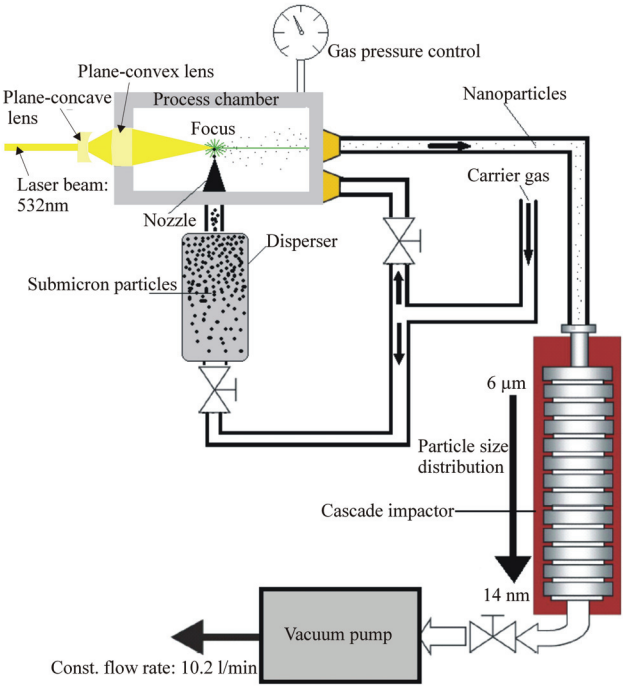

Fig. 1 Layout of the experimental set-up.

For alignment of the beam, a plane-concave lens (focal-length: 100 mm) and a plane-convex lens (focal-length: 80 mm) were put in series reaching a theoretical focal diameter of about 15 µm. The pulse energy was varied in the range of 12 to 48 mJ, reaching fluences of 6.8 to 27 kJ cm^{-2}, respectively. The pulsed laser beam was focused through a window into the process chamber directly above the feedstock particles outlet of the nozzle. The gas pressure (carrier gases: N_2 or Ar) inside the process chamber was controlled using a manometer.

The feedstock material, provided by a micro powder supplier, was put into the disperser, which dispersed the submicron particles through the nozzle into the chamber. A maximum submicron particle mass flow rate is 3.2 g/min. In this case, the feedstock particles fed into the chamber had a diameter of 0.5 – 2 µm during the investigations.

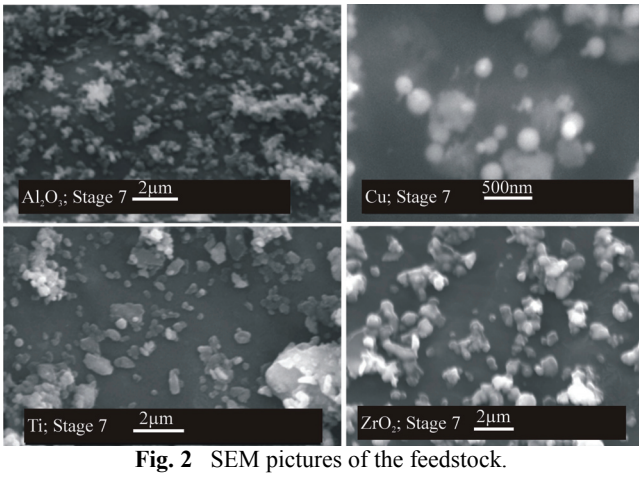

Fig. 2 SEM pictures of the feedstock.

The submicron particles and refined nanoparticles were separated on 12 stages of the cascade impactor and collected on aluminum foil in every experiment. The ELPI allows a direct monitoring of the particle size distribution and total particle number concentration. The particle size distribution can be monitored at 1 Hz during the running laser process.

In figure 2, SEM pictures of the submicron particles before refinement are shown, which demonstrate the real size distribution and the irregular morphology.

4. Results

A successive increase of the pulse energy (in 12 mJ steps) was tuned at the laser source to determine the influence of the pulse energy on the productivity.

In figures 3 and 4, the results on the fragmentation of microparticles are shown for the ceramic materials (ZrO_2, Al_2O_3) and the metal materials (Cu, Ti). The total particle number concentration with an aerodynamic diameter of 14 nm increased up to maximum values of about 1.5E+08 cm^{-3} (Ti) and 1.35E+08 cm^{-3} (ZrO_2), when the pulse energy was increased from 12 mJ to 48 mJ (fig. 3 and 4). Using higher pulse energies than 36 mJ the particle number concentration (with a particle size below 100 nm) could not increase during the experiments with Ti (see figure 3). An upper limit of total nanoparticle number is reached.

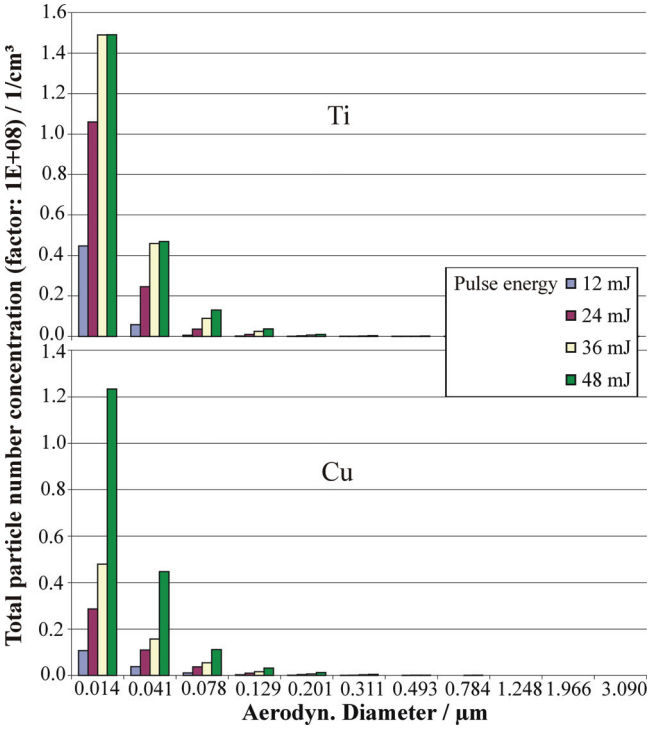

Fig. 3 Influence of the pulse energy on the particle size distribution of metal nanoparticles (carrier gas: N_2, gas pressure inside the chamber: 200kPa, pressure of the particle flow rate: 75kPa)

The productivity upper limit of the used system depends on the feed rate value of the feedstock material. The mass flow rate of primary nanoparticles (d_{ae} < 100 nm) could be increased with the increase of the pulse energy, but not the particle number concentration of the Ti nanoparticles with an aerodynamic diameter of 14 nm.

As a result of these experiments, the fragmentation of Ti microparticles saturates at the laser pulse energy above 36 mJ.

The strongest influence of pulse energy variation on the total nanoparticle number was observed during the experiments with Cu and ZrO_2. An increase of the pulse energy from 36 mJ to 48 mJ caused an increase of the productivity of more than 100% for Cu, and nearly 50% for ZrO_2.

The interaction of a single laser pulse with a particle also depends on the density of the material used. For example, an increase in the pulse energy of about 12 mJ (36 to 48 mJ) changes the particle number concentration of the most bonded particles with an aerodynamic diameter particle size of 14 nm by the following factors:

- → Cu (δ = 8.9 g/cm³) = increase of particle number concentration: 0.75 E+08 cm^{-3}
- → Al_2O_3 (δ = 4,0 g/cm³) = increase of particle number concentration: 0.08 E+08 cm^{-3}

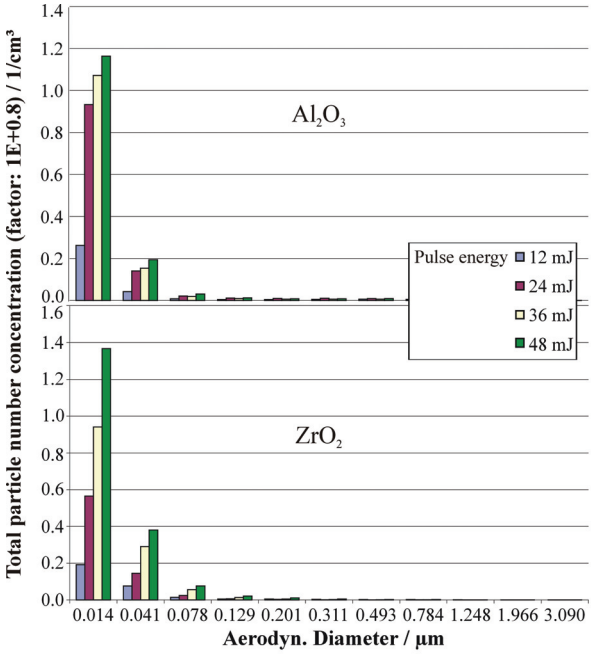

Fig. 4 Influence of the pulse energy on the particle size distribution of ceramic nanoparticles (carrier gas: N_2, gas pressure inside the chamber: 200kPa, pressure of the particle flow rate: 75kPa)

We determined a correlation of the laser fluence effect and the material density, relating to higher amount of particle number concentration (particle density) when using materials with higher density (see also figure 7).

Furthermore, the degree of laser absorptivity of the used feedstock material also depends on the laser wavelength and influences the particle size distribution and the total particle number concentration value, especially when using Cu.

In the next step, we observed the quality of the LAM process especially with regard to the particle size distribution before and after the interaction of the laser pulse with the raw particles when using Cu and Al_2O_3 as feedstock material.

The efficiency of the LAM process could be optimised by using a flow-optimised process chamber. The particles larger than 0.1 µm were filtered by an impactor after abla-

tion in order to separate the raw material (>100 nm) from the LAM nano-aerosol (fig. 5 and 6).

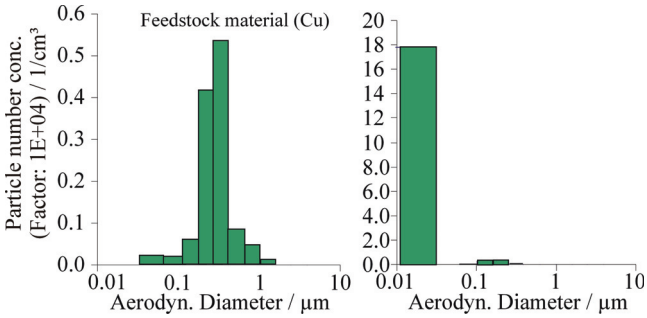

Fig. 5 Particle size distribution of Cu before (left) and after laser cracking (right) (pulse energy: 12 mJ, carrier gas: N_2, gas pressure inside the chamber: 200 kPa, pressure of the particle flow rate: 75 kPa)

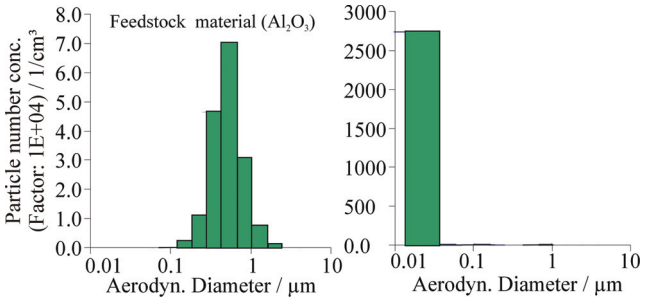

Fig. 6 Particle size distribution of Al_2O_3 before (left) and after laser cracking (right) (pulse energy: 12 mJ, carrier gas: N_2, gas pressure inside the chamber: 200 kPa, pressure of the particle flow rate: 75 kPa)

The mean aerodynamic diameter of the Cu feedstock material (5.0E+03 cm^{-3} at 500 nm) (see fig. 5 left diagramm) could be decreased significantly to 14 nm, and the particle number concentration could be increased by two orders of magnitude up to values of about 1.8E+05 cm^{-3} (see fig. 5, right diagramm).

When using Al_2O_3 as a feedstock material, the efficiency is even higher. The aerodynamic diameter of 700 nm could be decreased to 14 nm, and a higher particle number concentration up to a value of about 2.7 E+07 cm^{-3} compared to a particle number concentration of 7.0E+04 cm^{-3} of the raw material (fig. 6) is achieved. The efficiency of LAM processes also depends on the reflectivity of the used materials (Cu and Al_2O_3, normal reflectivity: Cu = 0.61 and Al_2O_3 = 0.85) [11, 18] concerning to the applied wavelength (λ= 532 nm). It was observed that the production rate mainly depends on the particle size distribution of the feedstock material. With regard to figure 4 highest particle number concentration of the feedstock material Al_2O_3 has been measured on impactor stage 8 (d_{ae} = 0.784 µm) compared to Cu (impactor stage 7; d_{ae} = 0.493 µm).

Furthermore, the applied mass flow rates per pulse energy of all four different raw materials were determined. In figure 7 mass flow rate dependence from pulse energy for the metallic and ceramic nanoparticles (aerodyn. diameter < 100 nm) are shown. The cross section for laser beam absorption is constant depending on the focal diameter. The mass flow rates of laser-generated nanoparticles were about 2 – 3 mg/h when using pulse energy of 12 mJ and increased to values of 4.5 mg/h (Al_2O_3) and 24.5 mg/h (Cu) when using 48mJ. The proportionally increase of the mass flow rates per pulse energy by the following factor (in Δ mg/h / mJ): Al_2O_3 = 0.1; ZrO_2 = 0.3; Ti = 0.4 and Cu = 0.6 is determined.

The maximum mass production rate per hour was determined with the metallic material Cu.

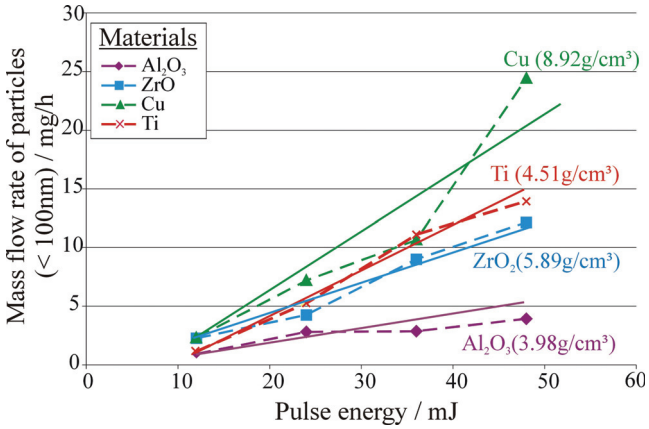

Fig. 7 Influence of the pulse energy on nanoparticles (d < 100 nm) and density of the material on the mass flow rate (Carrier gas: N_2, gas pressure inside the chamber: 200 kPa, pressure of the particle flow rate: 75 kPa)

The mass ablation efficiency of laser-based refinement of submicron-particles is about 40 – 50% with regard to overall captured particles using the ELPI. The mass ablation efficiency of the experimental set-up also depends on the system for impaction and separation and the construction of the process chamber and the disperser. More investigations may optimise controlled transportation of the micro-powder and powder stream focusing.

The average particle number concentration <100 nm of all four different materials was determined. The results are listed in table 1. Overall, the particle number concentration (< 100 nm) increased with the increase of the pulse energy. The highest production efficiency for nanoparticles < 100 nm could be reached with Ti. In comparison to Al_2O_3 the half pulse energy is necessary for the generation of the same amount of particle number concentration.

Table 1 Average particle number concentration (< 100 nm) using different pulse energies

Material	Particle number concentration x $10^7/cm^{-3}$			
	12mJ	24mJ	36mJ	48mJ
Al_2O_3	3.12	10.90	12.40	13.90
Cu	1.56	4.33	6.91	17.90
ZrO_2	2.82	7.34	12.90	18.20
Ti	5.11	13.40	20.40	20.90

During a trial period of 1 h, nanoparticles < 100 nm were generated with an applied laser pulse energy of 2.6 kJ. An energy per mass of about 106 J/mg was used for Cu

nanoparticles, for Ti nanoparticles: 185 J/mg, for ZrO_2 nanoparticles: 216 J/mg and for Al_2O_3 nanoparticles: 648 J/mg.

In the next step of the investigations, the use of nitrogen and argon as carrier gas was compared with regard to nanoparticle productivity. In summary, the application of Argon resulted in 27% to 56% higher productivity compared to nitrogen when the particle number concentration of all used materials (fig. 8) were determined using a pulse energy of 48 mJ.

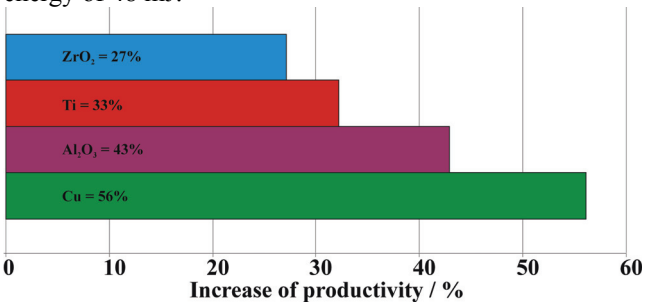

Fig. 8 Influence of argon on the increased productivity compared to the use of nitrogen (pulse energy : 48 mJ, gas pressure inside the chamber: 200 kPa, pressure of the particle flow rate: 75 kPa

The efficiency of the nanoparticle generation could also be influenced by the pressure of the particle flow rate.

The highest productivity of particle number concentration (d_{ae} < 100 nm) was reached when using Ti as feedstock material. When using Cu as feedstock material the highest mass flow rate of 24.5 mg/h was determined. Both were analyzed using the same process conditions: pressure of the particle flow rate = 75 kPa; feedstock particle flow rate = 3.2 g/min, argon as gas type; pulse energy = 48 mJ.

In figure 9 a SEM picture of impacted primary Ti nanoparticles on Aluminum-folio is shown collected with the ELPI. These nanoparticles have spherical and partial square-edged shape. Moreover, with the EDX of these nanoparticles Ti was determined as the main element of the al-folio.

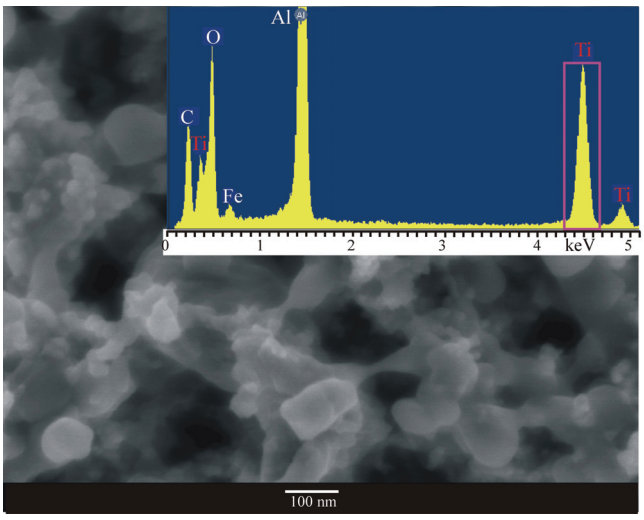

Fig. 9 SEM picture and an EDX analysis of impacted primary Ti nanoparticles on Al-folio

5. Summary

The presented LAM process shows good promising results for the fragmentation of submicron particles for nanoparticle generation using an experimental set-up with only a few components.

It has been demonstrated that the process parameters like pulse energy and the gas type have a strong influence on the productivity and the efficiency of the nanoparticle generation from metallic (Ti, Cu) and ceramic (Al_2O_3, ZrO_2) submicron particles.

The highest productivity of refined nanoparticles (with an aerodynamic diameter smaller than 100 nm) has been reached for Ti (with a particle number concentration of 1.5E+08 cm^{-3}) using a pulse energy of 48 mJ, argon as a carrier gas with a pressure inside the process chamber of 200 kPa, and a pressure of 75 kPa for the particle flow rate (feedstock material mass flow rate: 3.2 g/min). However, the highest nanoparticles generation efficiency has been reached for Cu microparticles.

At present, stabilization of nanoparticles to prevent agglomeration in gaseous media is still a problem which should be solved for future investigations. Therefore, a chamber for polymer coating of the nanoparticles to prevent agglomeration is planned.

Overall, the observed influences on the productivity and the efficiency can be summarized as follows:

a) an increase of the laser pulse energy (from 12 mJ to 84 mJ) proportionally increases the nanoparticle number concentration for all investigated materials.
b) a higher effect of the pulse energy on the total increase of nanoparticle number concentration is observed for feedstock materials with higher densities.
c) when argon is used as an ambient gas, the refined nanoparticle number concentration is higher compared to nitrogen.

References

[1] A. Ebenau: Economic Perspectives of Nanotechnology: Economic Markets for tiny Particles. In: Nanotechnology in Chemistry – Experience meets Vision on 28/29 October 2002 in Mannheim.

[2] S. Breitung-Faes, A. Kwade: Mahlkörpereinfluss bei der Nanozerkleinerung in Rührwerkskugelmühlen. Chemie Ingenieur Technik, Vol. 78, Issue 9, p. 1339 (2006)

[3] S. Barcikowski, A. Hahn, A. V. Kabashin, B. N. Chichkov: Properties of Nanoparticles generated during Femtosecond laser machining in air and water. Appl. Phys. A. 87, 47-55 (2007)

[4] S. Barcikowski, N. Bärsch, M. Hustedt, R. Sattari, A. Ostendorf: Continuous Production and Online-Characterization of Nanoparticles from Ultrafast Laser Ablation and Laser Cracking. In: Proceedings of 23nd International Conference on Applications of Lasers and Electro-Optics ICALEO 2005, 31.Oct.-03.Nov, Miami, CA, USA, p.6. (Conference Proceedings)

[5] Nichols, W. T., Malyavanatham, G., Henneke, D. E., Brock, J. R., Becker, M. F., Keto, J. W., Glicksmann, H. D.: Gas and pressure dependence for the mean size of nanoparticles produced by laser ablation of flowing

aerosols. In: Journal of Nanoparticle Research. 2000, Vol. 2, pp. 141 – 145

[6] A. Semerok, C. Chaléard, V. Detalle, J.-L. Lacour, P. Mauchien, P. Meynadier, C. Nouvellon, B. Sallé, P. Palianov, M. Perdrix, G. Petite: Experimental investigations of laser ablation efficiency of pure metals with femto, pico and nanosecond pulses. Appl. Surface Science 138-139 (1999), 311-314.

[7] Ausanio, G., Barone, A.C., Iannotti, V., Lanotte, L., Amoroso, S., Bruzzese, R., Vitello, M.: Magnetic and morphological characteristics of nickel nanoparticles films produced by femtosecond laser ablation. In: Applied Physics Letters. 2004, Vol. 85, Nr. 18, pp. 4103 – 4105

[8] M.F. Becker, J.R. Brock, Hong Cai, D.E. Henneke, J.W. Keto, Jaemyoung Lee, W.T. Nichols and H.D. Glicksmann: Metal nanoparticles generated by laser ablation, NanoStructured Materials, Vol. 10, No. 5, pp.853-863, 1998

[9] H. Chai, N. Chaudhary, J. Lee, M.F. Becker, J.R. Brock, J.W. Keto : Generation of metal nanoparticles by laser ablation of microspheres. Journal Aerosol Sci. Vol. 29, No. 5/6, pp. 627-636, 1998

[10] Lee, J., Becker, M. F., Keto, J. W.: Dynamics of laser ablation of microparticles prior to nanoparticle generation. In: Journal of Applied Physics. 2001, Vol. 89, Nr. 12, pp. 8146 – 8152

[11] D. Jang, B. Oh, D. Kim: Visualization of microparticle explosion and flow field in nanoparticle synthesis by pulsed laser ablation. Department of Mechanical Engineering, POSTECH, Pohang 790-784, Korea, Applied Physics A 79, 1149-1151, 2004

[12] Nikolay, D.; Kollenberg, W.; Deller, K.; Oswald, M.; Tontrup, C.: Manufacturing and properties of ZTA-Ceramics with nanoscaled ZrO_2. Ceramic forum international, Berichte der Deutschen Keramischen gesellschaft e.V., 83, No. 4, 2006

[13] Harmathy, P.; Amende, W.; Zechmeister, H.; et al: Zur Erzeugung von metallischen Verschleißschutzschichten mit hohem Karbidanteil unter Einsatz von infraroten Laserstrahlen. Konferenz-Einzelbeitrag: Laser 87, 1987, S. 448 - 452

[14] König, W.; Treppe, F.: Perspektiven der Laserrandschichtbehandlung von Warmarbeitswerkzeugen – Einordnung und Abgrenzung der Verfahrensvarianten. Konferenz-Einzelbericht: Neue Werkstoffe und Verfahren für Werkzeuge, 1989, S. 315 - 326

[15] Nowotny, S.: Beschichten, Reparieren und Generieren durch Präzisions-Auftragschweißen mit Laserstrahlen. Vakuum in Forschung und Praxis, Nr. 1 (2002), S. 33 – 37

[16] Kimberley, W.: Taking a shine to Mercedes. Automotive Engineer 29 (2004) 3, S. 44-46

[17] Dahmann, D.; Riediger, J.; Schlatter, A.; Wiedensohler, S.; Graff, M.; Grosser, Hojgr, M.; Horn, H.-G.; Jing, L.; Matter, U.; Monz, C.; Mosimann, T.; Stein, H.; Wehner, B.; Wieser, U.: Intercomparison of mobility sizers (MPS). Gefahrstoffe-Reinhaltung der Luft; p. 423-428, 61, Nr. 10, October 2001

[18] Gillner, A.; Hartmann, C.: Kombinationsverfahren zur Herstellung keramischer und schwer zerspanbarer Mikrokomponenten. Abschlussbericht des Verbundprojektes KOMBILAS; Fraunhofer Institut für Lasertechnik Aachen; 2005

(Received: November 20, 2007, Accepted: February 25, 2008)